SICE-ICASE International Joint Conference 2006
Oct. 18-21, 2006 in Bexco, Busan, Korea

Passivity-based Synchronized Control of Teleoperation with Power Scaling

Hisanosuke KAWADA and Toru NAMERIKAWA

Graduate School of Natural Science and Technology, Kanazawa University, Kanazawa, Japan
(Tel : +81-76-234-4848; E-mail: hisa@scl.ec.t.kanazawa-u.ac.jp and toru@t.kanazawa-u.ac.jp)

Abstract: This paper deals with the passivity-based synchronized control of teleoperation considering position tracking and power scaling. In the proposed method, the motion and the force relation between the master and slave robots can be specified freely. Using a passivity of the systems and Lyapunov stability methods, the asymptotic stability of teleoperation with communication delay and power scaling is proven. Several experimental results show the effectiveness of our proposed method.

Keywords: Teleoperation, Power scaling, Passivity-based synchronized control, Asymptotically stable

1. INTRODUCTION

Teleoperation system is the extension of a person's sensing and manipulation capability to remote environment. A typical teleoperation system consists of the master robot, the slave robot, the human operator, the remote environment and the communication line. If only the master motion and/or force are transmitted to the slave, the teleoperation system is called unilateral. If, in addition, the slave motion and/or force are transmitted to the master, the teleoperation system is called bilateral.

In bilateral teleoperation, the master and the slave are coupled via communication lines and communication delay is incurred in transmission of data between the master and slave sites. The delay in a closed loop system can destabilize the system. It is well known that the scattering transformation approach guarantees passivity of the communication line with any constant communication delay [1], [2]. As shown in [3], [4], this approach drives the velocity errors between the master and slave robots to zero, but can only guarantees the position tracking error to be bounded. Additionally, the scattering transformation is necessary to calculate the algebra loop. It is difficult to mount on a computer.

In [5], it is shown that multi passive systems with any constant communication delay can be synchronized. Moreover, the practical applicability of the result is demonstrated in the problem of teleoperation with any communication delay. Therefore, this approach guarantees position and velocity errors to zero without using scattering transformation.

In several tasks involving bilateral teleoperations, such as telesurgery and teleoperation of huge robotics for extra-vehicular activity in space application, the master and slave act at different scales and therefore, it is necessary that the motion and the force are transformed. This transformation is called as the power scaling [6]. In [6], it is shown that a scaling of exchanged power can be performed without affecting passivity. However, in this case, the asymptotic stability of position tracking errors is not guaranteed, because the scattering transformation approach is used.

In this paper, we propose the passivity-based synchronized control of teleoperation considering position tracking and power scaling. In the proposed method, the motion and the force relation between the master and slave robots can be specified freely. Using a passivity of the systems and Lyapunov stability methods the asymptotic stability of teleoperation with communication delay and power scaling is proven. Several experimental results show the effectiveness of our proposed method.

2. DYNAMICS OF TELEOPERATION

Assuming absence of friction and other disturbances, the master and slave robot dynamics for n-degree-of-freedom are given as [7]

$$\begin{aligned} \boldsymbol{M_m}(q_m)\ddot{\boldsymbol{q}}_{\boldsymbol{m}} + \boldsymbol{C_m}(q_m,\dot{q}_m)\dot{\boldsymbol{q}}_{\boldsymbol{m}} + \boldsymbol{g_m}(q_m) &= \boldsymbol{\tau_m} + \boldsymbol{F_{op}} \\ \boldsymbol{M_s}(q_s)\ddot{\boldsymbol{q}}_{\boldsymbol{s}} + \boldsymbol{C_s}(q_s,\dot{q}_s)\dot{\boldsymbol{q}}_{\boldsymbol{s}} + \boldsymbol{g_s}(q_s) &= \boldsymbol{\tau_s} - \boldsymbol{F_{env}}, \end{aligned} \quad (1)$$

where the subscript "m" and "s" show the master and the slave indexes respectively, $\boldsymbol{q}_m,\ \boldsymbol{q}_s \in R^{n\times1}$ are the joint angle vectors, $\dot{\boldsymbol{q}}_{\boldsymbol{m}},\ \dot{\boldsymbol{q}}_{\boldsymbol{s}}, \in R^{n\times1}$ are the joint velocity vectors, $\boldsymbol{\tau_m},\ \boldsymbol{\tau_s} \in R^{n\times1}$ are the input torque vectors, $\boldsymbol{F_{op}} \in R^{n\times1}$ is the operational torque vectors applied to the master robot by human operator, $\boldsymbol{F_{env}} \in R^{n\times1}$ is the environmental torque vectors applied to the environment by the slave robot, $\boldsymbol{M_m},\ \boldsymbol{M_s} \in R^{n\times n}$ are the symmetric and positive definite inertia matrices, $\boldsymbol{C_m}\dot{\boldsymbol{q}}_{\boldsymbol{m}},\ \boldsymbol{C_s}\dot{\boldsymbol{q}}_{\boldsymbol{s}} \in R^{n\times1}$ are the centripetal and Coriolis torque vectors and $\boldsymbol{g_m},\ \boldsymbol{g_s} \in R^{n\times1}$ are the gravitational torque vectors.

It is well known that the above equations have several fundamental properties as follows.

Property 1: The inertia matrix $\boldsymbol{M}(q)$ is symmetric and positive definite and there exist some positive constant m_1 and m_2 such that

$$0 < m_1\boldsymbol{I} \le \boldsymbol{M}(q) \le m_2\boldsymbol{I}. \quad (2)$$

Property 2: Under an appropriate definition of the matrix $\boldsymbol{C}(q,\dot{q})$, the matrix $\boldsymbol{N} = \dot{\boldsymbol{M}}(q) - 2\boldsymbol{C}(q,\dot{q})$ is skew symmetric such that

$$\boldsymbol{N}^T = -\boldsymbol{N}, \quad \boldsymbol{x}^T\boldsymbol{N}\boldsymbol{x} = 0. \tag{3}$$

where $\boldsymbol{x} \in R^{n\times 1}$ is any vector.

3. CONTROL OBJECTIVES

We would like to design $\boldsymbol{\tau_m},\ \boldsymbol{\tau_s}$ in (1) to achieve a synchronized teleoperation with power scaling.

We define the position tracking error with power scaling between the master and slave robots as

$$\begin{cases} \boldsymbol{e_m}(t) = \alpha^{-1}\boldsymbol{q_s}(t-T) - \boldsymbol{q_m}(t) \\ \boldsymbol{e_s}(t) = \alpha\boldsymbol{q_m}(t-T) - \boldsymbol{q_s}(t). \end{cases} \tag{4}$$

where $\alpha \in R$ is positive and any scaling factors. The teleoperation system is said to be synchronized if

$$\begin{cases} \boldsymbol{e}_i(t) \to 0 \quad as \quad t \to \infty \quad i = m, s \\ \dot{\boldsymbol{e}}_i(t) \to 0 \quad as \quad t \to \infty \quad i = m, s. \end{cases} \tag{5}$$

4. CONTROL DESIGN

To achieve the synchronized teleoperation system, we design the master and slave controllers.

4.1 Passivity-based Nonlinear Compensation

The master and slave input torque are given as [5],

$$\begin{aligned} \boldsymbol{\tau}_m = {} & -\boldsymbol{M_m}(q_m)\boldsymbol{\Lambda}\dot{\boldsymbol{q}}_{\boldsymbol{m}} - \boldsymbol{C_m}(\dot{q}_m, q_m)\boldsymbol{\Lambda}\boldsymbol{q_m} \\ & + \boldsymbol{g_m}(q_m) + \boldsymbol{F_m} \\ \boldsymbol{\tau}_s = {} & -\boldsymbol{M_s}(q_s)\boldsymbol{\Lambda}\dot{\boldsymbol{q}}_{\boldsymbol{s}} - \boldsymbol{C_s}(\dot{q}_s, q_s)\boldsymbol{\Lambda}\boldsymbol{q_s} \\ & + \boldsymbol{g_s}(q_s) + \boldsymbol{F_s}, \end{aligned} \tag{6}$$

where $\boldsymbol{F_m}$ and $\boldsymbol{F_s}$ are the additional input torque required for synchronized control in next section and $\boldsymbol{\Lambda} \in R^{n\times n}$ is a positive definite diagonal gain matrix.

Substituting (6) into (1), the master and slave robot dynamics are represented as

$$\begin{cases} \boldsymbol{M_m}(q_m)\dot{\boldsymbol{r}}_{\boldsymbol{m}} + \boldsymbol{C_m}(q_m,\dot{q}_m)\boldsymbol{r_m} = \boldsymbol{F_m} + \boldsymbol{F_{op}} \\ \boldsymbol{M_s}(q_s)\dot{\boldsymbol{r}}_{\boldsymbol{s}} + \boldsymbol{C_s}(q_s,\dot{q}_s)\boldsymbol{r_s} = \boldsymbol{F_s} - \boldsymbol{F_{env}}, \end{cases} \tag{7}$$

where the vector $\boldsymbol{r_m}$ and $\boldsymbol{r_s}$ are the new outputs of the master and slave robots and are given as

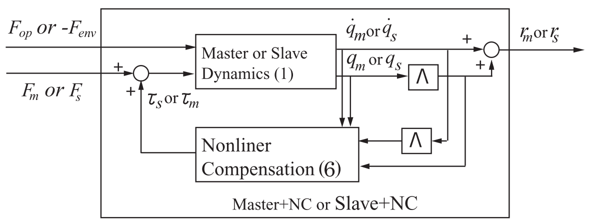

Fig. 1 The master and slave dynamics with nonlinear compensation

$$\begin{cases} \boldsymbol{r_m}(t) = \dot{\boldsymbol{q}}_m(t) + \boldsymbol{\Lambda}\boldsymbol{q}_m(t) \\ \boldsymbol{r_s}(t) = \dot{\boldsymbol{q}}_s(t) + \boldsymbol{\Lambda}\boldsymbol{q}_s(t). \end{cases} \tag{8}$$

There are defined by linear combinations of the joint angle vectors and the joint velocity vectors. Fig. 1 shows a block diagram of the master and slave robots with nonlinear compensation.

Then we have the following lemma.

Lemma 1: Consider the systems described by (7). Define the inputs of the master and slave robot dynamics as $\boldsymbol{\tau'_m} = \boldsymbol{F_m} + \boldsymbol{F_{op}}$ and $\boldsymbol{\tau'_s} = \boldsymbol{F_s} - \boldsymbol{F_{env}}$ and the outputs as $\boldsymbol{r_m}$ and $\boldsymbol{r_s}$ respectively. Then, the systems with the above input and outputs (Fig. 1) are passive such that.

$$\int_0^t \boldsymbol{r_i}^T(z)\boldsymbol{\tau'_i}(z)dz \geq -\beta, \quad i = m, s. \tag{9}$$

Proof: Define a positive definite function for the systems as

$$V_i(r_i(t)) = \frac{1}{2}\boldsymbol{r_i}^T(t)\boldsymbol{M_i}(q_i)\boldsymbol{r_i}(t), \quad i = m, s. \tag{10}$$

The derivative of this function along trajectories of the systems are given by

$$\begin{aligned} \dot{V}_i &= \frac{1}{2}\boldsymbol{r_i}^T\dot{\boldsymbol{M}}_{\boldsymbol{i}}\boldsymbol{r_i} + \boldsymbol{r_i}^T\boldsymbol{M_i}\dot{\boldsymbol{r}}_{\boldsymbol{i}} \\ &= \frac{1}{2}\underbrace{\boldsymbol{r_i}^T\{\dot{\boldsymbol{M}}_{\boldsymbol{i}} - 2\boldsymbol{C_i}\}\boldsymbol{r_i}}_{=0 \quad \texttt{property 2}} + \boldsymbol{r_i}^T\boldsymbol{\tau'_i} \\ &= \boldsymbol{r_i}^T\boldsymbol{\tau'_i}, \quad i = m, s. \end{aligned} \tag{11}$$

Then the master and slave robot dynamics guarantee the passivity as follows.

$$\begin{aligned} \int_0^t \boldsymbol{r_i}(z)^T\boldsymbol{\tau'_i}(z)dz &= V_i(r_i(t)) - V_i(r_i(0)) \\ &\geq -V(r_i(0)), \quad i = m, s. \end{aligned} \tag{12}$$

■

Using nonlinear compensation as (6), the master and slave dynamics are passive with respect to the output (8) that contains both position and velocity information. Thus the teleoperation can be controlled in the passivity framework for position and velocity signals by the new output.

4.2 Synchronized Control Law with Power Scaling

We propose the synchronized control law with power scaling as follows,

$$\begin{cases} \boldsymbol{F_m}(t) = \boldsymbol{K}(\alpha^{-1}\boldsymbol{r_s}(t-T) - \boldsymbol{r_m}(t)) \\ \boldsymbol{F_s}(t) = \boldsymbol{K}(\alpha\boldsymbol{r_m}(t-T) - \boldsymbol{r_s}(t)), \end{cases} \tag{13}$$

where $\boldsymbol{K} \in R^{n\times n}$ is a positive definite diagonal gain matrix, T is a constant communication delay. This control law has a very simple structure compared

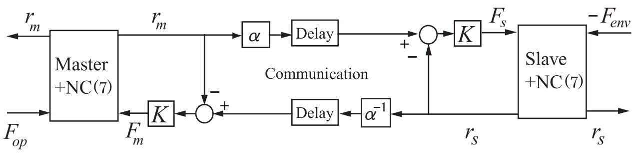

Fig. 2 The synchronization control architecture with power scaling

with the scattering based control in [4]. Fig. 1 shows a block diagram of teleoperation system with power scaling. The "Master+NC" and "Slave+NC" show the master's and slave's reduced dynamics in (7). The power scaling factors are located to both communication lines. The proposed control structure is also symmetric, i.e. the robots, the controllers and the scaling factors are in same form.

5. STABILITY ANALYSIS

In this section we analyze the proposed synchronized control law with a power scaling previously and show that the control objectives are successfully fulfilled. In the stability analysis that follows, we assume that

1. The operator and the environment can be modeled as passive systems with $\boldsymbol{r_m}$ and $\boldsymbol{r_s}$ as inputs respectively.
2. The operational and the environmental torque $\boldsymbol{F_{op}}$ and $\boldsymbol{F_{env}}$ are bounded by functions of the signals $\boldsymbol{r_m}$ and $\boldsymbol{r_s}$ respectively.
3. All signals belong to L_{2e}, the extended L_2 space.

Theorem 1: Consider the nonlinear teleoperation with power scaling described by (7) and (13). Then all signals in the system are bounded and the position tracking errors given by (4) $\boldsymbol{e_m}$,$\boldsymbol{e_s}$ and its derivatives $\dot{\boldsymbol{e}}_{\boldsymbol{m}}$, $\dot{\boldsymbol{e}}_{\boldsymbol{s}}$ are asymptotically stable. Therefore the teleoperation system is synchronized and power scaled.

Proof: Define a positive definite function for the system as

$$\begin{aligned} V_{ms}(x(t)) &= \alpha \boldsymbol{r_m}^T(t)\boldsymbol{M_m}(q_m)\boldsymbol{r_m}(t) + \alpha^{-1}\boldsymbol{r_s}^T(t)\boldsymbol{M_s}(q_s)\boldsymbol{r_s}(t) \\ &+\alpha \boldsymbol{e_m}^T(t)\boldsymbol{\Lambda K e_m}(t) + \alpha^{-1}\boldsymbol{e_s}^T(t)\boldsymbol{\Lambda K e_s}(t) \\ &+2\alpha^{-1}\int_0^t \left\{\boldsymbol{F_{env}}^T(z)\boldsymbol{r_s}(z)\right\}dz \\ &+2\alpha\int_0^t \left\{-\boldsymbol{F_{op}}^T(z)\boldsymbol{r_m}(z)\right\}dz \\ &+\int_{t-T}^t \left\{\alpha \boldsymbol{r_m}^T(z)\boldsymbol{K r_m}(z) + \alpha^{-1}\boldsymbol{r_s}^T(z)\boldsymbol{K r_s}(z)\right\}dz, \end{aligned} \tag{14}$$

where $\boldsymbol{M_m}$ and $\boldsymbol{M_s}$ are positive definite (by property 1), α is positive, $\boldsymbol{K}$ and $\boldsymbol{\Lambda}$ are positive definite diagonal matrices. The operator and the environment are passive (by assumption). Hence

$$2\alpha^{-1}\int_0^t \left\{\boldsymbol{F_{env}}^T(z)\boldsymbol{r_s}(z)\right\}dz \geq 0, \tag{15}$$

$$2\alpha\int_0^t \left\{-\boldsymbol{F_{op}}^T(z)\boldsymbol{r_m}(z)\right\}dz \geq 0. \tag{16}$$

Thus the function V_{ms} is positive definite. The derivative of this function along trajectories of the system with the property 2 are given by

$$\begin{aligned} \dot{V}_{ms} =& 2\alpha \boldsymbol{r_m}^T\boldsymbol{F_m} + 2\alpha^{-1}\boldsymbol{r_s}^T\boldsymbol{F_s} \\ &+ \alpha \boldsymbol{r_m}^T\boldsymbol{K r_m} - \alpha^{-1}\boldsymbol{r_s}^T(t-T)\boldsymbol{K r_s}(t-T) \\ &+ \alpha^{-1}\boldsymbol{r_s}^T\boldsymbol{K r_s} - \alpha \boldsymbol{r_m}^T(t-T)\boldsymbol{K r_m}(t-T) \\ &+ 2\alpha \boldsymbol{e_m}^T\boldsymbol{\Lambda K}\dot{\boldsymbol{e}}_{\boldsymbol{m}} + 2\boldsymbol{e_s}^T\boldsymbol{\Lambda K}\dot{\boldsymbol{e}}_{\boldsymbol{s}}. \end{aligned} \tag{17}$$

Using the facts that

$$\begin{aligned} &\alpha \boldsymbol{r_m}^T\boldsymbol{K r_m} - \alpha^{-1}\boldsymbol{r_s}^T(t-T)\boldsymbol{K r_s}(t-T) \\ &\quad = \{\alpha \boldsymbol{r_m} + \boldsymbol{r_s}(t-T)\}^T\boldsymbol{K}\{\boldsymbol{r_m} - \alpha^{-1}\boldsymbol{r_s}(t-T)\} \end{aligned} \tag{18}$$

$$\begin{aligned} &\alpha^{-1}\boldsymbol{r_s}^T\boldsymbol{K r_s} - \alpha \boldsymbol{r_m}^T(t-T)\boldsymbol{K r_m}(t-T) \\ &\quad = \{\alpha^{-1}\boldsymbol{r_s} + \boldsymbol{r_m}(t-T)\}^T\boldsymbol{K}\{\boldsymbol{r_s} - \alpha \boldsymbol{r_m}(t-T)\}, \end{aligned} \tag{19}$$

Then we have

$$\begin{aligned} \dot{V}_{ms} =& 2\alpha \boldsymbol{r_m}^T\boldsymbol{F_m} + 2\alpha^{-1}\boldsymbol{r_s}^T\boldsymbol{F_s} \\ &-\{\alpha \boldsymbol{r_m} + \boldsymbol{r_s}(t-T)\}^T\boldsymbol{K}\{\alpha^{-1}\boldsymbol{r_s}(t-T) - \boldsymbol{r_m}\} \\ &-\{\alpha^{-1}\boldsymbol{r_s} + \boldsymbol{r_m}(t-T)\}^T\boldsymbol{K}\{\alpha \boldsymbol{r_m}(t-T) - \boldsymbol{r_s}(t)\} \\ &+2\alpha \boldsymbol{e_m}^T\boldsymbol{\Lambda K}\dot{\boldsymbol{e}}_{\boldsymbol{m}} + 2\alpha^{-1}\boldsymbol{e_s}^T\boldsymbol{\Lambda K}\dot{\boldsymbol{e}}_{\boldsymbol{s}}. \end{aligned} \tag{20}$$

Substituting (13) into (20), we get

$$\begin{aligned} \dot{V}_{ms} =& -(\alpha^{-1}\boldsymbol{r_s}(t-T) - \boldsymbol{r_m})^T\alpha\boldsymbol{K}(\alpha^{-1}\boldsymbol{r_s}(t-T) - \boldsymbol{r_m}) \\ &-(\alpha \boldsymbol{r_m}(t-T) - \boldsymbol{r_s})^T\alpha^{-1}\boldsymbol{K}(\alpha \boldsymbol{r_m}(t-T) - \boldsymbol{r_s}) \\ &+2\alpha \boldsymbol{e_m}^T\boldsymbol{\Lambda K}\dot{\boldsymbol{e}}_{\boldsymbol{m}} + 2\alpha^{-1}\boldsymbol{e_s}^T\boldsymbol{\Lambda K}\dot{\boldsymbol{e}}_{\boldsymbol{s}}. \end{aligned}$$

Substituting (8) and using (4), it can be rewritten as

$$\begin{aligned} \dot{V}_{ms} =& -(\dot{\boldsymbol{e}}_{\boldsymbol{m}} + \boldsymbol{\Lambda e_m})^T\alpha\boldsymbol{K}(\dot{\boldsymbol{e}}_{\boldsymbol{m}} + \boldsymbol{\Lambda e_m}) \\ &- (\dot{\boldsymbol{e}}_{\boldsymbol{s}} + \boldsymbol{\Lambda e_s})^T\alpha^{-1}\boldsymbol{K}(\dot{\boldsymbol{e}}_{\boldsymbol{s}} + \boldsymbol{\Lambda e_s}) \\ &+ 2\alpha \boldsymbol{e_m}^T\boldsymbol{\Lambda K}\dot{\boldsymbol{e}}_{\boldsymbol{m}} + 2\alpha^{-1}\boldsymbol{e_s}^T\boldsymbol{\Lambda K}\dot{\boldsymbol{e}}_{\boldsymbol{s}} \\ \\ =& -\dot{\boldsymbol{e}}_{\boldsymbol{m}}^T\alpha\boldsymbol{K}\dot{\boldsymbol{e}}_{\boldsymbol{m}} - \boldsymbol{e_m}^T\alpha\boldsymbol{\Lambda K \Lambda e_m} \\ &- \dot{\boldsymbol{e}}_{\boldsymbol{s}}^T\alpha^{-1}\boldsymbol{K}\dot{\boldsymbol{e}}_{\boldsymbol{s}} - \boldsymbol{e_s}^T\alpha^{-1}\boldsymbol{\Lambda K \Lambda e_s}. \end{aligned} \tag{21}$$

Thus the derivative of the Lyapunov function $\dot{V}_{ms}$ is negative semi- definite.

To show the uniformly continuity of $\dot{V}_{ms}$, we consider the derivative of $\dot{V}_{ms}$ as follows,

$$\begin{aligned} \ddot{V}_{ms} =& -2\ddot{\boldsymbol{e}}_{\boldsymbol{m}}^T\alpha\boldsymbol{K}\dot{\boldsymbol{e}}_{\boldsymbol{m}} - 2\dot{\boldsymbol{e}}_{\boldsymbol{m}}^T\alpha\boldsymbol{\Lambda K \Lambda e_m} \\ &- 2\ddot{\boldsymbol{e}}_{\boldsymbol{s}}^T\alpha^{-1}\boldsymbol{K}\dot{\boldsymbol{e}}_{\boldsymbol{s}} - 2\dot{\boldsymbol{e}}_{\boldsymbol{s}}^T\alpha^{-1}\boldsymbol{\Lambda K \Lambda e_s}. \end{aligned} \tag{22}$$

The $\dot{V}_{ms}$ is uniformly continuous, if the $\ddot{\boldsymbol{e}}_{\boldsymbol{m}}, \ddot{\boldsymbol{e}}_{\boldsymbol{s}}, \dot{\boldsymbol{e}}_{\boldsymbol{m}}, \dot{\boldsymbol{e}}_{\boldsymbol{s}}$, $\boldsymbol{e_m}$ and $\boldsymbol{e_s}$ are bounded. Since V_{ms} is lower-bounded by zero and $\dot{V}_{ms}$ is negative semi-definite, we can conclude that,

$$
\begin{aligned}
\boldsymbol{r_m}^T \alpha \boldsymbol{M_m} \boldsymbol{r_m} &\leq V_{ms}(x(0)) \\
\boldsymbol{r_s}^T \alpha^{-1} \boldsymbol{M_s} \boldsymbol{r_s} &\leq V_{ms}(x(0)) \\
\boldsymbol{e_m}^T \alpha \boldsymbol{\Lambda K} \boldsymbol{e_m} &\leq V_{ms}(x(0)) \\
\boldsymbol{e_s}^T \alpha^{-1} \boldsymbol{\Lambda K} \boldsymbol{e_s} &\leq V_{ms}(x(0)).
\end{aligned}
$$

Using the fact that the inertia matrices $\boldsymbol{M_m}$ and $\boldsymbol{M_m}$ are lower bounded by Property 1, the signals $\boldsymbol{r_m}, \boldsymbol{r_s}, \boldsymbol{e_m}$ and $\boldsymbol{e_s}$ are bounded. Note that Laplace transform of (8) yields strictly proper, exponentially stable, transfer function between $\boldsymbol{r_m}, \boldsymbol{r_s}$ and $\boldsymbol{q_m}, \boldsymbol{q_s}$ is given as,

$$
\boldsymbol{Q_i}(s) = \begin{bmatrix} \frac{1}{s+\lambda_1} & \cdots & 0 \\ \vdots & \ddots & \vdots \\ 0 & \cdots & \frac{1}{s+\lambda_n} \end{bmatrix} \boldsymbol{R_i}(s) \quad , i = m, s, \tag{23}
$$

where "s" is the Laplace variable, the $\boldsymbol{R_i}(s)$ and $\boldsymbol{Q_i}(s)$ are the Laplace transform of the $\boldsymbol{r_i}(t)$ and $\boldsymbol{q_i}(t)$ respectively. Since $\boldsymbol{r_m}, \boldsymbol{r_s} \in \mathcal{L}_\infty$ and (23), it is easy to see that $\dot{\boldsymbol{q}}_{\boldsymbol{m}}(t), \dot{\boldsymbol{q}}_{\boldsymbol{s}}(t), \boldsymbol{q_m}(t), \boldsymbol{q_s}(t) \in \mathcal{L}_\infty$ and $\dot{\boldsymbol{e}}_{\boldsymbol{m}}, \dot{\boldsymbol{e}}_{\boldsymbol{s}} \in \mathcal{L}_\infty$. As the operational and the environmental torque are bounded by function of the signals $\boldsymbol{r_m}, \boldsymbol{r_s}$ respectively, $\boldsymbol{F_{op}}$ and $\boldsymbol{F_{env}}$ are also bounded. From (1), the master and slave acceleration are bounded which given us that $\ddot{\boldsymbol{e}}_{\boldsymbol{m}}, \ddot{\boldsymbol{e}}_{\boldsymbol{s}} \in \mathcal{L}_\infty$.

Thus $\ddot{V}_{ms}$ is bounded and $\dot{V}_{ms}$ is uniformly continuous. Applying Barbalt's Lemma [8] we can see that $\dot{V}_{ms} \to 0$ as $t \to \infty$. The signals $\boldsymbol{e_m}, \boldsymbol{e_s}, \dot{\boldsymbol{e}}_{\boldsymbol{m}}$ and $\dot{\boldsymbol{e}}_{\boldsymbol{s}}$ are asymptotically stable. Therefore the teleoperation system is synchronized and power scaled. ■

In the steady state, we can show that the contact torque is transmitted to the master side.

Proposition 1: Consider the nonlinear teleoperation with power scaling described by (7) and (13). The following relationship is achieved in the steady state

$$
\ddot{\boldsymbol{q}}_{\boldsymbol{i}}(t) = \dot{\boldsymbol{q}}_{\boldsymbol{i}}(t) = 0, \boldsymbol{q_i}(t) = \boldsymbol{q_i}, \quad i = m, s. \tag{24}
$$

Furthermore, we obtain that the scaled contact torque is accurately transmitted to the master robot side as follows

$$
\boldsymbol{F_{op}} = \boldsymbol{K\Lambda}(\alpha \boldsymbol{q_m} - \boldsymbol{q_s}) = \alpha^{-1} \boldsymbol{F_{env}} \tag{25}
$$

Proof: In the steady state (24), the master and slave dynamics (7) are reduced to

$$
\begin{cases} \boldsymbol{F_m} = -\boldsymbol{F_{op}} \\ \boldsymbol{F_s} = \boldsymbol{F_{env}} \end{cases}
$$

$$
\begin{cases} \boldsymbol{K\Lambda}(\alpha \boldsymbol{q_m} - \boldsymbol{q_s})\alpha^{-1} = \boldsymbol{F_{op}} \\ \boldsymbol{K\Lambda}(\alpha \boldsymbol{q_m} - \boldsymbol{q_s}) = \boldsymbol{F_{env}}. \end{cases}
$$

The above equations give

$$
\boldsymbol{F_{op}} = \boldsymbol{K\Lambda}(\alpha \boldsymbol{q_m} - \boldsymbol{q_s}) = \alpha^{-1} \boldsymbol{F_{env}}. \tag{26}
$$

Therefore the scaled contact torque is accurately transmitted to the master robot side. ■

Remark 1: From Theorem 1 and Proposition 1, we can conclude the following properties
• $\alpha > 1$: The motion/force of the slave robot is scaled up
• $\alpha < 1$: The motion/force of the slave robot is scaled down
• $\alpha = 1$: The slave robot is operated in a same scale
Additionally the asymptotic stability is guaranteed when the scaling factors is finite. Hence the proposed method can specify the scale of the motion and the force relationship between the master and slave robots freely.

6. EVALUATION BY CONTROL EXPERIMENTS

In this section, we verify the efficacy of the proposed teleoperation methodology. The experiments were carried out on a pair of identical direct-drive planar 2 links revolute-joint robots as shown in Fig. 3. We also measure the operational and the environmental torque (i.e. $\boldsymbol{F_{env}}, \boldsymbol{F_{op}}$ in (1)) using the force sensors. The inertia matrices, the Coriolis matrices and the gravitational torque are identified

$$
\begin{aligned}
\boldsymbol{M_i}(q_i) &= \begin{bmatrix} \theta_1 + 2\theta_3 \cos(q_2) & \theta_2 + \theta_3 \cos(q_2) \\ \theta_2 + \theta_3 \cos(q_2) & \theta_2 \end{bmatrix} \\
\boldsymbol{C_i}(q_i, \dot{q}_i) &= \begin{bmatrix} -\theta_3 \sin(q_2)\dot{q}_2 & -\theta_3 \sin(q_2)(\dot{q}_1 + \dot{q}_2) \\ \theta_3 \sin(q_2)\dot{q}_1 & 0 \end{bmatrix} \\
\boldsymbol{g_i}(q_i) &= 0, \quad i = m, s.
\end{aligned}
$$

The parameters of robots are given as follows

$$
\begin{aligned}
\theta_1 &= 0.3657[\mathtt{kgm^2}] \\
\theta_2 &= 0.0291[\mathtt{kgm^2}] \\
\theta_3 &= 0.0227[\mathtt{kgm}].
\end{aligned}
$$

Fig. 4 shows the experimental setup with a hard environment on the slave side. As a real-time operating system, we use RT-Linux and 1 [ms] sampling rate

Fig. 3 Experimental setup

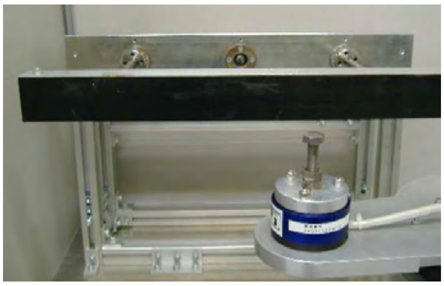

Fig. 4 Slave and environment

is obtained. All experiments have been done with a constant communication delay of 0.5 [s].

The controller parameters $\boldsymbol{K}$ and $\boldsymbol{\Lambda}$ are selected as follows

$$\boldsymbol{K} = \begin{bmatrix} 3 & 0 \\ 0 & 4 \end{bmatrix}, \quad \boldsymbol{\Lambda} = \begin{bmatrix} 1.5 & 0 \\ 0 & 2 \end{bmatrix}.$$

The scaling factor is selected as

$$\alpha = 2.$$

Hence we expect that the motion/torque of the slave robot is twice as much as those of the master robot.

Two kind of experimental conditions are given as follows.

- Case 1: Free space
- Case 2: Contact with environment

All experimental results show that the stability is guaranteed as Figs. 5-10.

Figs. 5 and 6 show the results of Case 1. From Fig. 5, The joint angle responses of the slave are about twice as much as those of the master as expected. Fig. 6 shows the result that the master responses are multiplied by two and the slave responses are shifted to 0.5[s] to cancel the communication delay. From Fig. 6, the joint angles of the slave accurately track those of the master and the synchronization with power scaling between the master and slave robots is achieved.

Figs. 7 - 10 show the results of Case 2. As shown in Figs. 7 and 8, when the slave robot is pushing the environment (2.5-12.5 [sec]), the contact torque is faithfully reflected to the operator. The operator can perceive the environment through the torque reflection. The environmental torque responses are about twice as much as operational torque responses as expected. Figs. 9 and 10 show the results that the master responses are multiplied by two and the slave responses are shifted to the left. From Figs. 9 and 10, the environmental torque on contact are accurately transmitted to the master side. When the slave dose not contact with environment and the operator forcing is negligible (12.5-18[sec]), the synchronization with power scaling between the master and slave robots is achieved.

In Fig. 9, there are some errors in the torque, but it is seems to be due to the substantial devise

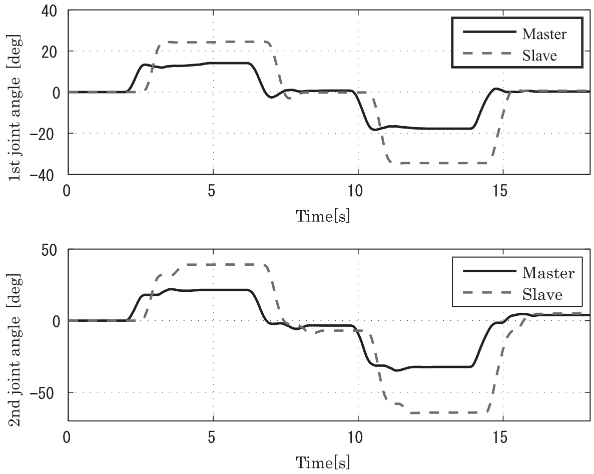

Fig. 5 Case 1: Time response in free space

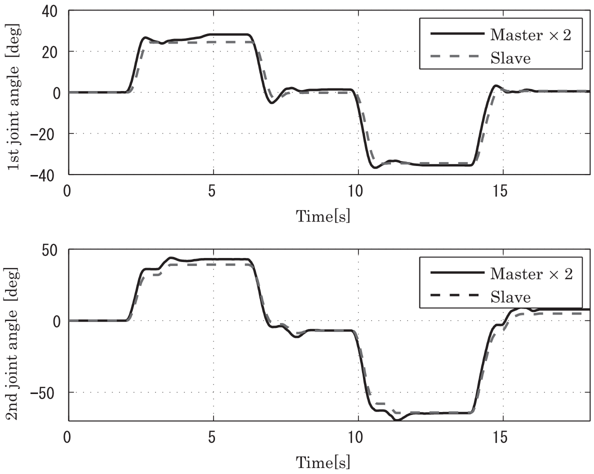

Fig. 6 Case 1: Time response in free space (Master response × 2)

coulomb friction of robots. These errors were not observed when a simulation without such a friction [9] is performed.

7. CONCLUSION

In this paper, we proposed the passivity-based synchronized control of teleoperation considering position tracking and power scaling. In the proposed method, the motion and the force relation between the master and slave robots can be specified freely. Using a passivity of the systems and Lyapunov stability methods the asymptotic stability of teleoperation with communication delay and power scaling was proven. Several experiments results showed the effectiveness of our proposed method.

REFERENCES

[1] R. J. Anderson and M. W. Spong, "Bilateral Control of Teleoperators with Time Delay,"

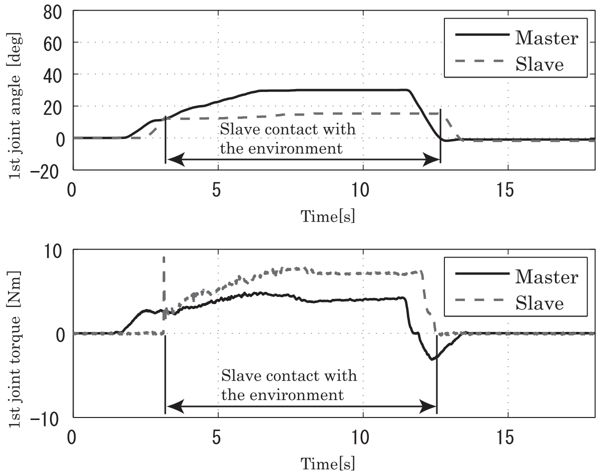

Fig. 7 Case 2: Contact with environment at 1st joint

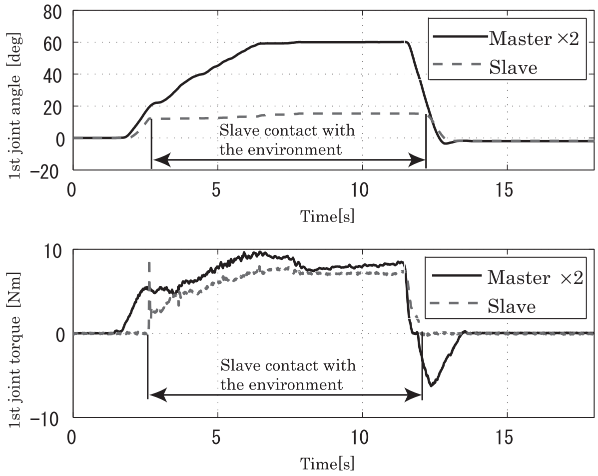

Fig. 9 Case 2: Contact with environment at 1st joint
(Master response × 2)

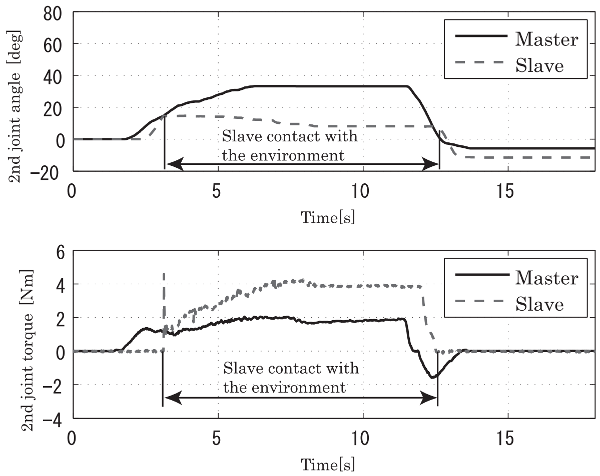

Fig. 8 Case 2: Contact with environment at 2nd joint

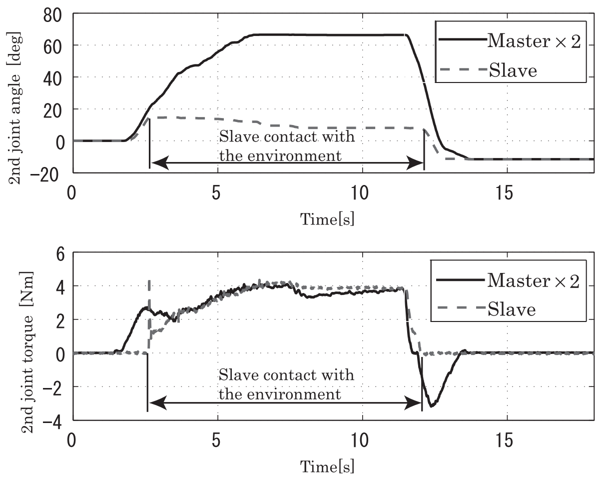

Fig. 10 Case 2: Contact with environment at 2nd joint
(Master response × 2)

IEEE Trans. on Automatatic Control, Vol. 34, No. 5, pp. 494-501, 1989.

[2] G. Niemeyer and J. -J. E. Slotine, "Telemanipulation with Time Delays," The Int. J. of Robotics Research, Vol 23, No.9, pp. 873-890, 2004.

[3] N. Chopra, M. W. Spong, R. Ortega and N. E. Barabanov, "On Position Tracking in Bilateral Teleoperation," Proc. of the ACC, pp. 5244-5249, 2004.

[4] T. Namerikawa and H. Kawada, "Symmetric Impedance Matched Teleoperation with Position Tracking", Proc. of the CDC, 2006 (to be published).

[5] N. Chopra and M. W. Spong,"On Synchronization of Networked Passive Systems with Time Delays and Application to Bilateral Teleoperation," Proc. of the SICE An. Conf. 2005, pp. 3424-3429, 2005.

[6] K. Kosuge, T. Itoh, I. Naniwa and T. Fukuda, "Passive Realization of Power scaling of Telemanipulator with Communication Time Delay," The JSME, Series C , Vol. 64, No. 621, pp. 304-309, 1998 (in Japanese).

[7] C. Canudas de Wit, B. Siciliano and G. Bastin, (Eds.), Theory of Robot Control, Springer-Verlag, 1996.

[8] H. K. Khalil, Nonlinear systems, second edition, Prentice-Hall, 1996.

[9] H. Kawada and T. Namerikawa, "Passivity-based Control of Teleoperation with Position Tracking," Technical Report of IEICE, Vol.106, No.136 (NLP2006-42), pp.49-54, 2006 (in Japanese).